Mediator and RNA polymerase II clusters associate in transcription-dependent condensates

Citation: Cho, Won-Ki et al. "Mediator and RNA polymerase II clusters associate in transcription-dependent condensates." Science 361, 6400 (July 2018): 412-415 © 2018 Academic Press

As Published: http://dx.doi.org/10.1126/science.aar4199

Publisher: American Association for the Advancement of Science (AAAS)

Persistent URL: https://hdl.handle.net/1721.1/123696

Version: Author's final manuscript: final author's manuscript post peer review, without publisher's formatting or copy editing

Title:

Mediator and RNA polymerase II clusters associate in transcription-dependent condensates

One sentence summary:

Critical components of transcription machinery, Mediator and RNA polymerase II, form stable, condensate-like, transcription-dependent clusters in living stem cells.

Authors:

Won-Ki Cho[1,*], Jan-Hendrik Spille[1,*], Micca Hecht[1], Choongman Lee[1], Charles Li[2,3], Valentin Grube[1,4], Ibrahim I. Cisse[1,‡]

Affiliations:

[1] Department of Physics,[2] Department of Biology, MIT, Cambridge, MA 02139, US

[3] Whitehead Institute for Biomedical Research, Cambridge, MA 02139, US

[4] Department of Physics, LMU Munich, Geschwister Scholl Platz 1, 80539 Munich, Germany

* equal contribution

‡ to whom correspondence should be addressed: icisse@mit.edu

Abstract:

Models of gene control have emerged from genetic and biochemical studies, with limited consideration of the spatial organization and dynamics of key components in living cells. Here we used live cell super-resolution and light sheet imaging to study the organization and dynamics of the Mediator coactivator and RNA polymerase II (Pol II) directly. Mediator and Pol II each form small transient and large stable clusters in living embryonic stem cells. Mediator and Pol II are colocalized in the stable clusters, which associate with chromatin, have properties of phase-separated condensates and are sensitive to transcriptional inhibitors. We suggest that large clusters of Mediator, recruited by transcription factors at large or clustered enhancer elements, interact with large Pol II clusters in transcriptional condensates in vivo.

Main text:

A conventional view of eukaryotic gene regulation is that transcription factors, bound to enhancer DNA elements, recruit coactivators such as the Mediator complex, which is thought to interact with RNA Polymerase II (Pol II) at the promoter (*1-5*). This model is supported by a large body of molecular genetic and biochemical evidence, yet the direct interaction of Mediator and Pol II has not been observed and characterized in living cells (*6*). Using super-resolution (*7-9*) and light sheet imaging (*10*), we studied the organization and dynamics of endogenous Mediator and Pol II in live mouse embryonic stem cells (mESCs). We directly tested whether Pol II and Mediator interact in a manner consistent with condensate formation (*11-13*), quantitatively characterized their biophysical properties, and considered the implications of these observations for transcription regulation in living mammalian cells.

To visualize Mediator and Pol II in live cells, we generated mESC lines with endogenous Mediator and Pol II labeled with Dendra2, a green-to-red photo-convertible fluorescent protein (**Materials and Methods**, **Fig. S1** and **S2**). We performed live cell super-resolution, and found that Mediator forms clusters (**Fig. 1A, Fig. S3**) with a range of dynamic temporal signatures. Mediator exists in a population of transient small (~100nm) clusters (**Fig. 1B**) with an average lifetime of 11.1 ± 0.9 s (**Fig. 1G**, mean ± s.e.m. from 36 cells), comparable to transient Pol II clusters observed here (**Fig. 1D, 1E** and **1H**) and previously in differentiated cell types (*14, 15*). In addition, we observed that both Mediator and Pol II form a populations (~14 per cell) of large clusters (>300nm), each comprised of ~200-400 molecules, that are temporally stable (lasting the full acquisition window of the live cell super-resolution imaging) (**Fig.1C**, **1F-H**, **Fig. S4, Fig. S5, Fig. S6**).

We tested the extent to which these clusters depend on the stem cell state. The mESCs were subjected to a protocol (*16*) to differentiate them into Epiblast-like cells (EpiLC) within 24h (**Materials and Methods** and **Fig. S7**). There was no apparent effect of differentiation on the population of transient clusters, consistent with previous observations that transient clusters persist in differentiated cell types (*14, 15*). However, there was a decrease in both the size and number of stable clusters along the course of differentiation (**Fig 1I** and **1J, Fig. S8**), suggesting that these stable clusters are prone to change as cells differentiate.

We focused on the stable clusters of Mediator and Pol II and investigated whether they are colocalized. We generated mESCs with endogenous Mediator and Pol II tagged with JF646-HaloTag (*15, 17*) and Dendra2, respectively (**Materials and Methods**, **Fig. S1** and **S2**). Direct imaging of both JF646-Mediator (**Fig. 2A)** and Dendra2-Pol II (**Fig. 2B)** showed bright spots of large accumulations in the nucleus, which corresponded to stable Pol II clusters according to subsequent super-resolution imaging of Dendra2-Pol II in the same nuclei (**Fig 2C).** The same observations were made with Dendra2-Mediator (**Fig. S9**). Out of 143 Mediator clusters imaged by dual color light sheet imaging (**Fig. 2D–2F)** 129 (90%) had a co-localizing Pol II cluster (**Fig. 2G** and **2H**, also **Materials and Methods** and **Fig. S9**). We conclude that these Mediator and Pol II clusters colocalize in live mESCs.

Previous studies have shown that high densities of Mediator are located at enhancer clusters called super-enhancers (SEs) and that some are disrupted by loss of the BET bromodomain protein BRD4, which is a cofactor associated with Mediator (*18, 19*). We found that treatment of mESCs with JQ1, a drug that causes loss of BRD4 from enhancer chromatin, dissolved transient and stable clusters of both Mediator and Pol II clusters (**Fig. 2I-N** and **Fig. S10**).

After transcription initiation, Pol II transcribes a short distance (~100bp), pauses, and is released to continue elongation when phosphorylated by CDK9 (*20*). We hypothesized that inhibition of CDK9 might selectively affect the Pol II stable clusters. We observed that upon incubation with DRB Pol II stable clusters dissolved but Mediator stable clusters remained (**Fig. 2O**). Quantification of Mediator/Pol II colocalization revealed that DRB incubation progressively decreased the fraction of Mediator stable clusters that colocalize with Pol II (**Fig. 2P**). This effect could be reversed when DRB was washed out; the colocalization fraction recovered completely. These results imply that the association between Mediator and Pol II clusters may be hierarchical, with upstream enhancer recruitment controlling both clusters but downstream transcription inhibition selectively affecting Pol II clusters.

We characterized the long-term dynamics of stable clusters using lattice light sheet imaging in live mESCs (**Movie S1** and **S2**). We observed that clusters can merge upon contact (**Fig. 3A-3D**, **Movie S1 and S2**). The timescale of coalescence was very rapid, comparable to our full volumetric acquisition frame rate (15s time interval). The added-up intensity of the two precursor clusters was close to that of the newly merged cluster (**Fig. 3E Fig. S11**). These biophysical dynamics are reminiscent of biomolecular condensates *in vivo* (*21*).

In addition to coalescence, *in vivo* condensates had rapid turnover of the molecular components shown by fast recovery in Fluorescence Recovery after Photobleaching (FRAP) assays, and were sensitive to a non-specific aliphatic alcohol, 1,6-hexanediol (*21*). Our FRAP analyses of clusters revealed very rapid dynamics and turnover of their components: 60 percent of the Mediator and 90 percent of Pol II components were exchanged within ~10 seconds within clusters (**Fig. 3F-3H**). Moreover, the treatment of mESCs with 1,6-hexanediol resulted in the

gradual dissolution of both Mediator and Pol II clusters (**Fig. 3I–3K** and **Fig. S12**). Together, these results suggest that the stable clusters are *in vivo* condensates of Mediator and Pol II.

We hypothesized that a phase separation model with induced condensation at the recruitment step of Mediator to enhancers would qualitatively account for the observations in this study (*22*). The model implies that the condensates are chromatin-associated and colocalize with enhancer-controlled active genes. We therefore tested these two specific implications. We tracked the diffusion dynamics of Mediator clusters by computing their mean squared displacement (MSD) as a function of time (N=6 cells). At short time scales, the cluster motion was sub-diffusive with an exponent $\alpha = 0.40 \pm 0.12$ (best fit ± s.e.m) (**Fig. S13**). This is the same exponent found in the sub-diffusional behavior of chromatin loci in eukaryotic cells (*23-27*). We also observed the same diffusional parameters when tracking a chromatin locus labeled by dCas9-based CARGO in mESCs (**Fig. S13)** (*23*). We concluded that clusters diffuse like chromatin-associated domains.

We hypothesized that clusters were in close physical proximity to actively transcribed genes that can be visualized by global run-on nascent RNA labeling with ethynyl uridine (EU) (**Fig. S14**). The run-on results showed that 2 minutes after DRB washout, virtually all Mediator clusters observed were proximal or overlapping with nascent RNA accumulations as imaged by Click-labelling of EU in fixed cells (**Fig. S14**). We also employed the MS2 endogenous RNA labeling system (*15, 28*) **(Materials and Methods** and **Fig. S15**) to investigate whether active transcription could be observed at *Esrrb*, one of the top SE-controlled genes in mESCs (*29*) (**Fig. 4A**), We observed bright foci consistent with nascent MS2-labeled gene loci, and confirmed the gene loci by dual color RNA FISH targeting the MS2 sequence and intronic regions of *Esrrb* (**Fig. S16**). Intronic FISH on 125 *Esrrb* loci from 82 fixed cells showed that 93% of *Esrrb* loci had a stable Mediator cluster nearby (within 1μm) but only ~22% of the loci colocalize with a stable

Mediator cluster, suggesting that the Mediator-bound enhancer only occasionally colocalizes with the gene (**Fig. S17**). The variability in colocalization may be explained by a dynamic kissing model, where a distal Mediator cluster colocalizes with the gene only at certain timepoints (**Fig. 4A**).

By dual-color 3D live-cell imaging with lattice light sheet microscopy, we found that some Mediator clusters were up to a micrometer away from the active *Esrrb* gene locus but in some instances directly colocalized with the gene (**Fig. 4B, 4C**). In addition, we directly observed the dynamic interaction between Mediator clusters and the gene locus, supporting the dynamic kissing model (**Fig. 4D, 4E** and **Fig. S18, Movie S3**). Tracking of loci in all 6 cells indicated that colocalization below our resolution limit of 300nm occurs in ~30% of the timepoints (**Fig. 4F**). However, even when they were not overlapping, the Mediator cluster and the gene loci moved as a pair through the nucleus (**Movie S3**), consistent with two adjacent regions anchoring to the same underlying chromatin domain. We propose that Mediator clusters form at the *Esrrb* super-enhancer and then interact occasionally and transiently with the transcription apparatus at the *Esrrb* promoter.

We find that Mediator and Pol II form large stable clusters in living cells and show that these have properties expected for biomolecular condensates. The condensate properties were evident through coalescence, rapid recovery in FRAP analysis, and sensitivity to Hexanediol. When considered in a model of phase separation based on scaffold-client relationships (*30*), it is possible that enhancer-associated Mediator forms a condensate and provides a "scaffold" for "client" RNA polymerase II molecules. The model we propose whereby large Mediator clusters at enhancers transiently kiss the transcription apparatus at promoters has a number of implications for gene control mechanisms. The presence of large Mediator clusters at some enhancers might

allow Mediator condensates to contact the transcription apparatus at multiple gene promoters simultaneously. The large size of the Mediator clusters may also mean that the effective distance of the enhancer-promoter DNA elements can be in the same order as the size of the clusters (>300nm) larger than the distance requirement for direct contact. We speculate that such clusters may help explain gaps of hundreds of nanometers that are found in previous studies measuring distances between functional enhancer-promoter DNA elements. Such cluster sizes also imply that perhaps some long-range interactions could go undetected in DNA interaction assays that depend on much closer physical proximity of enhancer and promoter DNA elements.

References and Notes

1. P. J. Robinson, M. J. Trnka, D. A. Bushnell, R. E. Davis, P. J. Mattei, A. L. Burlingame, R. D. Kornberg, Structure of a Complete Mediator-RNA Polymerase II Pre-Initiation Complex. *Cell* **166**, 1411-1422 e1416 (2016).
2. R. D. Kornberg, Mediator and the mechanism of transcriptional activation. *Trends Biochem Sci* **30**, 235-239 (2005).
3. C. T. Ong, V. G. Corces, Enhancer function: new insights into the regulation of tissue-specific gene expression. *Nat Rev Genet* **12**, 283-293 (2011).
4. K. M. Lelli, M. Slattery, R. S. Mann, Disentangling the many layers of eukaryotic transcriptional regulation. *Annu Rev Genet* **46**, 43-68 (2012).
5. B. L. Allen, D. J. Taatjes, The Mediator complex: a central integrator of transcription. *Nat Rev Mol Cell Biol* **16**, 155-166 (2015).
6. M. Levine, C. Cattoglio, R. Tjian, Looping back to leap forward: transcription enters a new era. *Cell* **157**, 13-25 (2014).
7. S. T. Hess, T. P. Girirajan, M. D. Mason, Ultra-high resolution imaging by fluorescence photoactivation localization microscopy. *Biophysical journal* **91**, 4258-4272 (2006).
8. M. J. Rust, M. Bates, X. Zhuang, Sub-diffraction-limit imaging by stochastic optical reconstruction microscopy (STORM). *Nature methods* **3**, 793-795 (2006).
9. E. Betzig, G. H. Patterson, R. Sougrat, O. W. Lindwasser, S. Olenych, J. S. Bonifacino, M. W. Davidson, J. Lippincott-Schwartz, H. F. Hess, Imaging intracellular fluorescent proteins at nanometer resolution. *Science (New York, N.Y.)* **313**, 1642-1645 (2006).
10. B. C. Chen, W. R. Legant, K. Wang, L. Shao, D. E. Milkie, M. W. Davidson, C. Janetopoulos, X. S. Wu, J. A. Hammer, 3rd, Z. Liu, B. P. English, Y. Mimori-Kiyosue, D. P. Romero, A. T. Ritter, J. Lippincott-Schwartz, L. Fritz-Laylin, R. D. Mullins, D. M. Mitchell, J. N. Bembenek, A. C. Reymann, R. Bohme, S. W. Grill, J. T. Wang, G. Seydoux, U. S. Tulu, D. P. Kiehart, E. Betzig, Lattice light-sheet microscopy: imaging molecules to embryos at high spatiotemporal resolution. *Science* **346**, 1257998 (2014).
11. D. Hnisz, K. Shrinivas, R. A. Young, A. K. Chakraborty, P. A. Sharp, A Phase Separation Model for Transcriptional Control. *Cell* **169**, 13-23 (2017).
12. T. Fukaya, B. Lim, M. Levine, Enhancer Control of Transcriptional Bursting. *Cell* **166**, 358-368 (2016).
13. Z. Liu, W. R. Legant, B. C. Chen, L. Li, J. B. Grimm, L. D. Lavis, E. Betzig, R. Tjian, 3D imaging of Sox2 enhancer clusters in embryonic stem cells. *Elife* **3**, e04236 (2014).
14. Cisse, II, I. Izeddin, S. Z. Causse, L. Boudarene, A. Senecal, L. Muresan, C. Dugast-Darzacq, B. Hajj, M. Dahan, X. Darzacq, Real-time dynamics of RNA polymerase II clustering in live human cells. *Science* **341**, 664-667 (2013).
15. W. K. Cho, N. Jayanth, B. P. English, T. Inoue, J. O. Andrews, W. Conway, J. B. Grimm, J. H. Spille, L. D. Lavis, T. Lionnet, Cisse, II, RNA Polymerase II cluster dynamics predict mRNA output in living cells. *Elife* **5**, (2016).
16. C. Buecker, R. Srinivasan, Z. Wu, E. Calo, D. Acampora, T. Faial, A. Simeone, M. Tan, T. Swigut, J. Wysocka, Reorganization of enhancer patterns in transition from naive to primed pluripotency. *Cell Stem Cell* **14**, 838-853 (2014).
17. J. B. Grimm, B. P. English, J. Chen, J. P. Slaughter, Z. Zhang, A. Revyakin, R. Patel, J. J. Macklin, D. Normanno, R. H. Singer, T. Lionnet, L. D. Lavis, A general method to improve fluorophores for live-cell and single-molecule microscopy. *Nat Methods* **12**, 244-250, 243 p following 250 (2015).
18. P. Filippakopoulos, J. Qi, S. Picaud, Y. Shen, W. B. Smith, O. Fedorov, E. M. Morse, T. Keates, T. T. Hickman, I. Felletar, M. Philpott, S. Munro, M. R. McKeown, Y. Wang, A. L. Christie, N. West, M. J. Cameron, B. Schwartz, T. D. Heightman, N. La Thangue, C. A.

French, O. Wiest, A. L. Kung, S. Knapp, J. E. Bradner, Selective inhibition of BET bromodomains. *Nature* **468**, 1067-1073 (2010).
19. J. Loven, H. A. Hoke, C. Y. Lin, A. Lau, D. A. Orlando, C. R. Vakoc, J. E. Bradner, T. I. Lee, R. A. Young, Selective inhibition of tumor oncogenes by disruption of super-enhancers. *Cell* **153**, 320-334 (2013).
20. N. F. Marshall, D. H. Price, Control of formation of two distinct classes of RNA polymerase II elongation complexes. *Molecular and cellular biology* **12**, 2078-2090 (1992).
21. Y. Shin, C. P. Brangwynne, Liquid phase condensation in cell physiology and disease. *Science (New York, N.Y.)* **357**, (2017).
22. B. R. Sabari, A. Dall'Agnese, A. Boija, I. A. Klein, E. L. Coffey, K. Shrinivas, B. J. Abraham, N. M. Hannett, A. V. Zamudio, J. C. Manteiga, C. H. Li, Y. E. Guo, D. S. Day, J. Schuijers, E. Vasile, S. Malik, D. Hnisz, T. I. Lee, I. I. Cisse, R. G. Roeder, P. A. Sharp, A. K. Chakraborty, R. A. Young, Coactivator condensation at super-enhancers links phase separation and gene control. (Science, in press)
23. B. Gu, T. Swigut, A. Spencley, M. R. Bauer, M. Chung, T. Meyer, J. Wysocka, Transcription-coupled changes in nuclear mobility of mammalian cis-regulatory elements. *Science* **359**, 1050-1055 (2018).
24. J. R. Chubb, S. Boyle, P. Perry, W. A. Bickmore, Chromatin motion is constrained by association with nuclear compartments in human cells. *Curr Biol* **12**, 439-445 (2002).
25. J. S. Lucas, Y. Zhang, O. K. Dudko, C. Murre, 3D trajectories adopted by coding and regulatory DNA elements: first-passage times for genomic interactions. *Cell* **158**, 339-352 (2014).
26. V. Dion, S. M. Gasser, Chromatin movement in the maintenance of genome stability. *Cell* **152**, 1355-1364 (2013).
27. S. C. Weber, A. J. Spakowitz, J. A. Theriot, Bacterial chromosomal loci move subdiffusively through a viscoelastic cytoplasm. *Phys Rev Lett* **104**, 238102 (2010).
28. E. Bertrand, P. Chartrand, M. Schaefer, S. M. Shenoy, R. H. Singer, R. M. Long, Localization of ASH1 mRNA particles in living yeast. *Mol Cell* **2**, 437-445 (1998).
29. W. A. Whyte, D. A. Orlando, D. Hnisz, B. J. Abraham, C. Y. Lin, M. H. Kagey, P. B. Rahl, T. I. Lee, R. A. Young, Master transcription factors and mediator establish super-enhancers at key cell identity genes. *Cell* **153**, 307-319 (2013).
30. S. F. Banani, H. O. Lee, A. A. Hyman, M. K. Rosen, Biomolecular condensates: organizers of cellular biochemistry. *Nature reviews. Molecular cell biology* **18**, 285-298 (2017).
31. D. M. Chudakov, S. Lukyanov, K. A. Lukyanov, Tracking intracellular protein movements using photoswitchable fluorescent proteins PS-CFP2 and Dendra2. *Nat Protoc* **2**, 2024-2032 (2007).
32. O. Bensaude, Inhibiting eukaryotic transcription: Which compound to choose? How to evaluate its activity? *Transcription* **2**, 103-108 (2011).
33. W. K. Cho, N. Jayanth, S. Mullen, T. H. Tan, Y. J. Jung, Cisse, II, Super-resolution imaging of fluorescently labeled, endogenous RNA Polymerase II in living cells with CRISPR/Cas9-mediated gene editing. *Sci Rep* **6**, 35949 (2016).
34. A. Serge, N. Bertaux, H. Rigneault, D. Marguet, Dynamic multiple-target tracing to probe spatiotemporal cartography of cell membranes. *Nature methods* **5**, 687-694 (2008).
35. J. O. Andrews, W. Conway, W. Cho, A. Narayanan, J. Spille, N. Jayanth, T. Inoue, S. Mullen, J. Thaler, Cisse, II, qSR: a quantitative super-resolution analysis tool reveals the cell-cycle dependent organization of RNA Polymerase I in live human cells. *Sci Rep* **8**, 7424 (2018).
36. M. Ester et al. (AAAI Press, Proceedings of the Second International Conference on Knowledge Discovery and Data Mining (KDD-96), 1996), pp. 226-231.

37. X. Darzacq, Y. Shav-Tal, V. de Turris, Y. Brody, S. M. Shenoy, R. D. Phair, R. H. Singer, In vivo dynamics of RNA polymerase II transcription. *Nat Struct Mol Biol* **14**, 796-806 (2007).
38. T. Lambert, L. Shao, LLSpy v0.3.7. *Zenodo*, (2017).
39. J. Schindelin, I. Arganda-Carreras, E. Frise, V. Kaynig, M. Longair, T. Pietzsch, S. Preibisch, C. Rueden, S. Saalfeld, B. Schmid, J. Y. Tinevez, D. J. White, V. Hartenstein, K. Eliceiri, P. Tomancak, A. Cardona, Fiji: an open-source platform for biological-image analysis. *Nat Methods* **9**, 676-682 (2012).
40. C. Y. Jao, A. Salic, Exploring RNA transcription and turnover in vivo by using click chemistry. *Proc Natl Acad Sci U S A* **105**, 15779-15784 (2008).
41. M. Ovesný, P. Křížek, J. Borkovec, Z. Švindrych, G. M. Hagen, ThunderSTORM: a comprehensive ImageJ plug-in for PALM and STORM data analysis and super-resolution imaging. *Bioinformatics* **30**, 2389-2390 (2014).
42. K. L. Tsai, C. Tomomori-Sato, S. Sato, R. C. Conaway, J. W. Conaway, F. J. Asturias, Subunit Architecture and Functional Modular Rearrangements of the Transcriptional Mediator Complex. *Cell* **158**, 463 (2014).
43. S. Sato, C. Tomomori-Sato, C. A. Banks, I. Sorokina, T. J. Parmely, S. E. Kong, J. Jin, Y. Cai, W. S. Lane, C. S. Brower, R. C. Conaway, J. W. Conaway, Identification of mammalian Mediator subunits with similarities to yeast Mediator subunits Srb5, Srb6, Med11, and Rox3. *J Biol Chem* **278**, 15123-15127 (2003).

Acknowledgements

We thank L. D. Lavis (HHMI/Janelia) and J. Grimm (HHMI/Janelia) for gift of the JF646-Halo dyes, E. Calo (MIT) for the wild-type R1 cells, and differentiation protocol. We thank J. Wysocka (Stanford) for the CARGO material. We thank R. Young (MIT) and members of the Young, Sharp and Chakraborty groups (MIT) for helpful discussions, and R. Young and J. Gore (MIT) for helpful comments on the manuscript. We acknowledge the students of the Cissé Lab rotation in the 2017 MBL Physiology course for participation in early aspects of Dendra2-Pol II characterization in mESCs and J.O. Andrews for assistance with the qSR analysis software. The lattice light sheet microscope was home built in the Cissé Lab at MIT Physics under license from HHMI, Janelia Research Campus, and we thank E. Betzig (HHMI/Janelia) and W. Legant (HHMI/Janelia) for their critical support in the process. FRAP experiments were performed at the W.M. Keck Microscopy Facility at the Whitehead Institute. **Funding:** This work was supported primarily by the NIH Director's New Innovator award #DP2CA195769 (to I.I.C), and also by the Pew Charitable Trusts through the PEW Biomedical Scholars Program grant (to I.I.C.). I.I.C is also supported by the NIH 4D Nucleome through NOFIC. J.-H.S. is supported by a postdoctoral fellowship from the German Research Foundation (DFG, SP1680/1-1). **Author contributions:** W.K.C., J.-H.S., and I.I.C. conceived and designed the study; W.K.C. and J.-H.S. performed experiments and analyzed data with help from M.H., C.Lee, and V.G.; M.H. cloned CRISPR repair templates and sgRNA plasmids and genotyped cell lines; C.Li conducted and analyzed the Western Blot and ChIP-seq assay. W.K.C., J.-H.S., and I.I.C. wrote the manuscript with input from all co-authors. I.I.C. supervised all aspects of the project. **Competing interests:** The authors declare that they have no competing interests. **Data and materials availability:** All data and materials will be provided upon reasonable request to the corresponding author. ChIP-seq data sets generated in

this study have been deposited in the Gene Expression Omnibus under accession number GSE115436. Other data described in the manuscript is presented in the Supplementary Material.

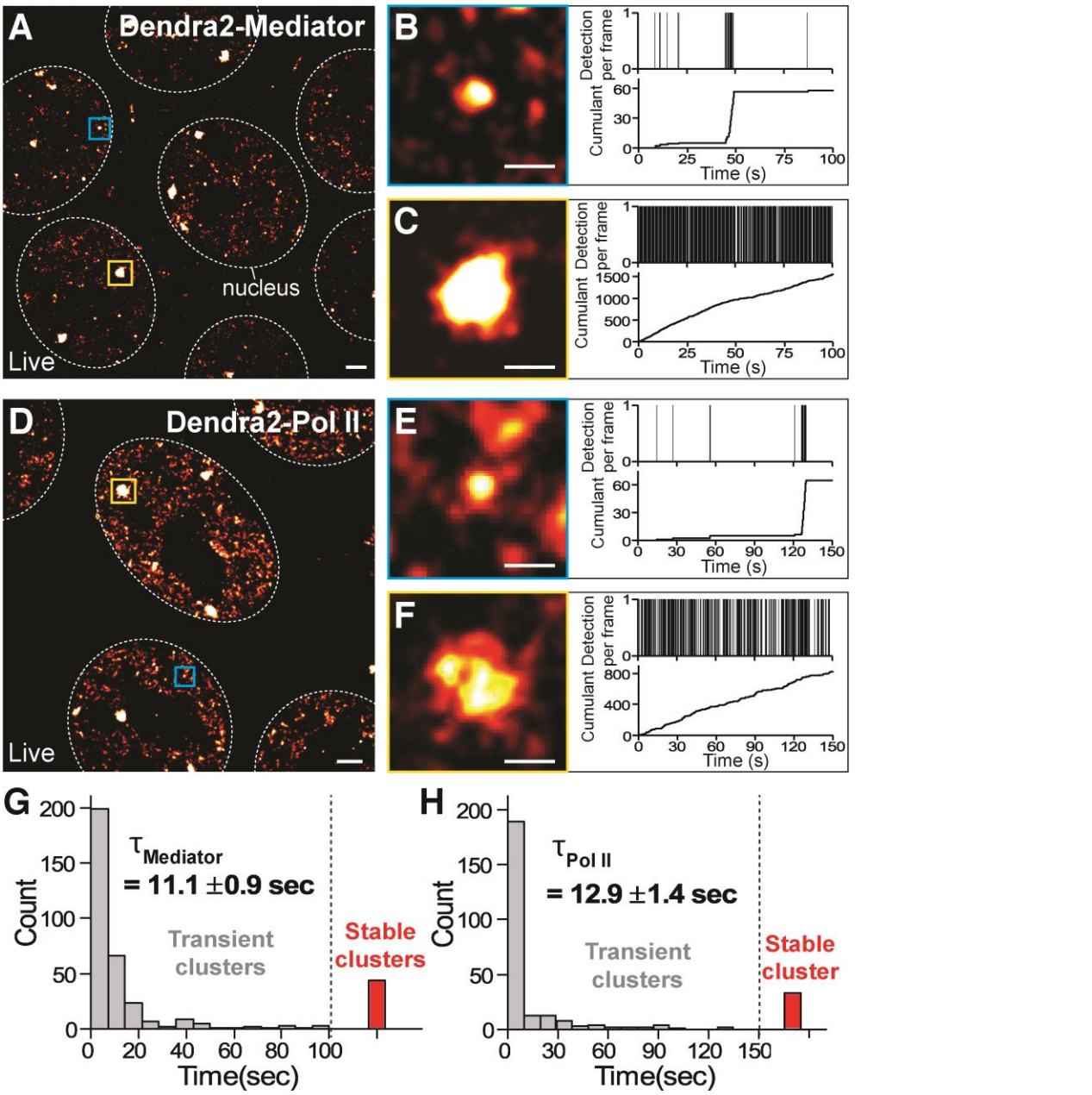

Fig. 1. Mediator and Pol II form transient and stable clusters in living mESCs.

(**A**) A super-resolution image of endogenous Mediator labeled with Dendra2 in living mESCs. (**B, C**) Representative super-resolved images of transient and stable Mediator clusters and corresponding tcPALM traces. (**D**) Super-resolution image of endogenous Pol II labeled with Dendra2 in living mESCs. (**E, F**) Representative super-resolution images of transient and stable Pol II clusters and corresponding tcPALM traces. (**G, H**) Lifetime distributions of Mediator and Pol II clusters, respectively. Red bars indicate stable clusters. Scale bars 1 μm in **A**, **D** and 500 nm in **B, C, E, F**.

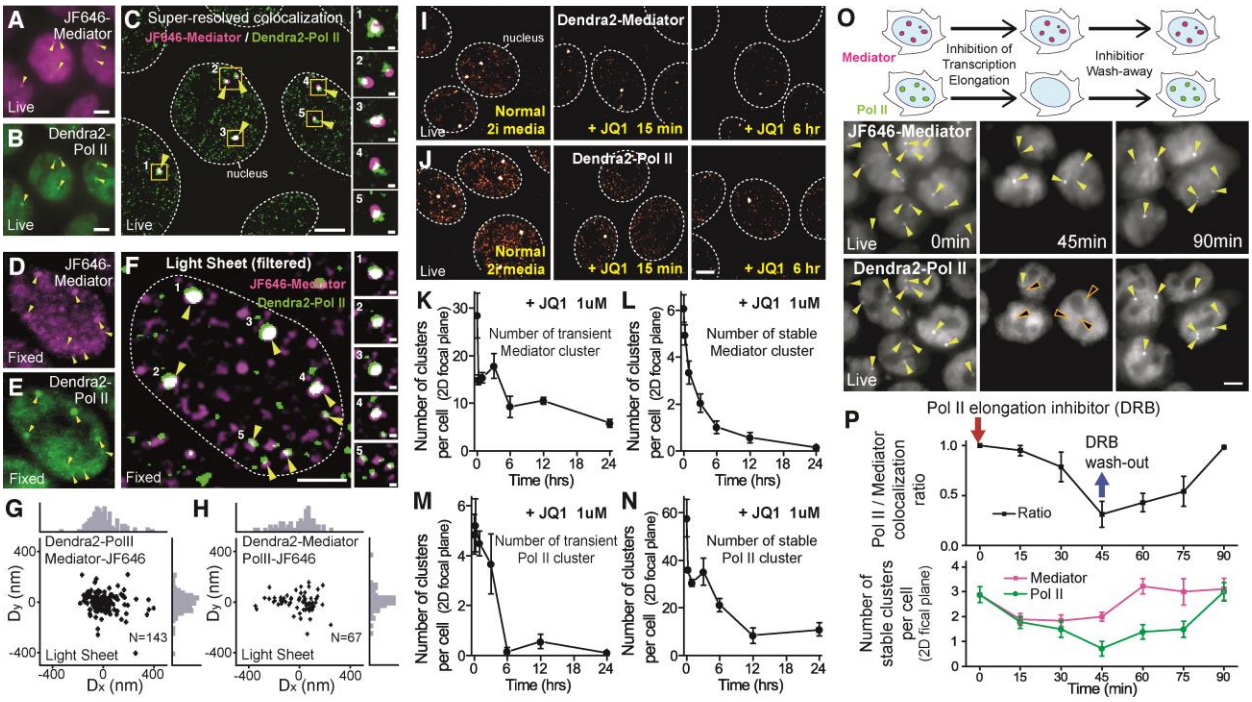

Fig. 2. Mediator and Pol II clusters colocalize in a transcription dependent manner.

(**A**) Live cell direct images of JF646-Mediator and (**B**) Dendra2-Pol II. Yellow arrowheads indicate stable clusters. (**C**) Super-resolution image of Dendra2-Pol II overlaid with a background-subtracted JF646-Mediator image. Insets 1-5 show Mediator and Pol II colocalization in clusters. (**D**) JF646-Mediator and (**E**) Dendra2-Pol II maximum intensity projections of a fixed cell imaged by lattice light sheet microscopy. (**F**) Overlay of background-subtracted images. Yellow arrowheads indicate clusters identified in the Dendra2-PolII channel. (**G**) Scatter plot of the distance from a Dendra2-Pol II cluster to the nearest JF646-Mediator cluster (N=143). Insets show histograms of the distances along the x- and y-axis. (**H**) Same analysis for clusters identified in the Dendra2-Mediator channel (N=67). (**I, J**) Super-resolution images of Dendra2-Mediator and Dendra2-Pol II under normal condition (left) and after 15 min (middle) or 6hr (right) incubation in 1µM JQ1. (**K, M**) The number of transient Mediator and Pol II clusters per cell in a 2D focal plane as a function of time after JQ1 addition.-(**L, N**) The number of stable Mediator and Pol II clusters per cell in a 2D focal plane. N=17-25 cells and N=14-24 cells at each JQ1 time point for Mediator and Pol II, respectively. (**O**) DRB treatment and wash-out experiments. DRB (100 µM) was added at 0 min and washed away after 45 min. Arrowheads indicate stable clusters identified in the JF646-Mediator channel. Black arrowheads in the middle panel (bottom) indicate Mediator clusters that did not colocalize with Pol II clusters. (**P**) Ratio (top) and absolute number (bottom) of clusters detected in the Pol II and Mediator channels per cell in 2D focal plane. N=9-15 cells were analyzed for each DRB incubation time point. Scale bars 2 µm in overview images, 200 nm in insets.

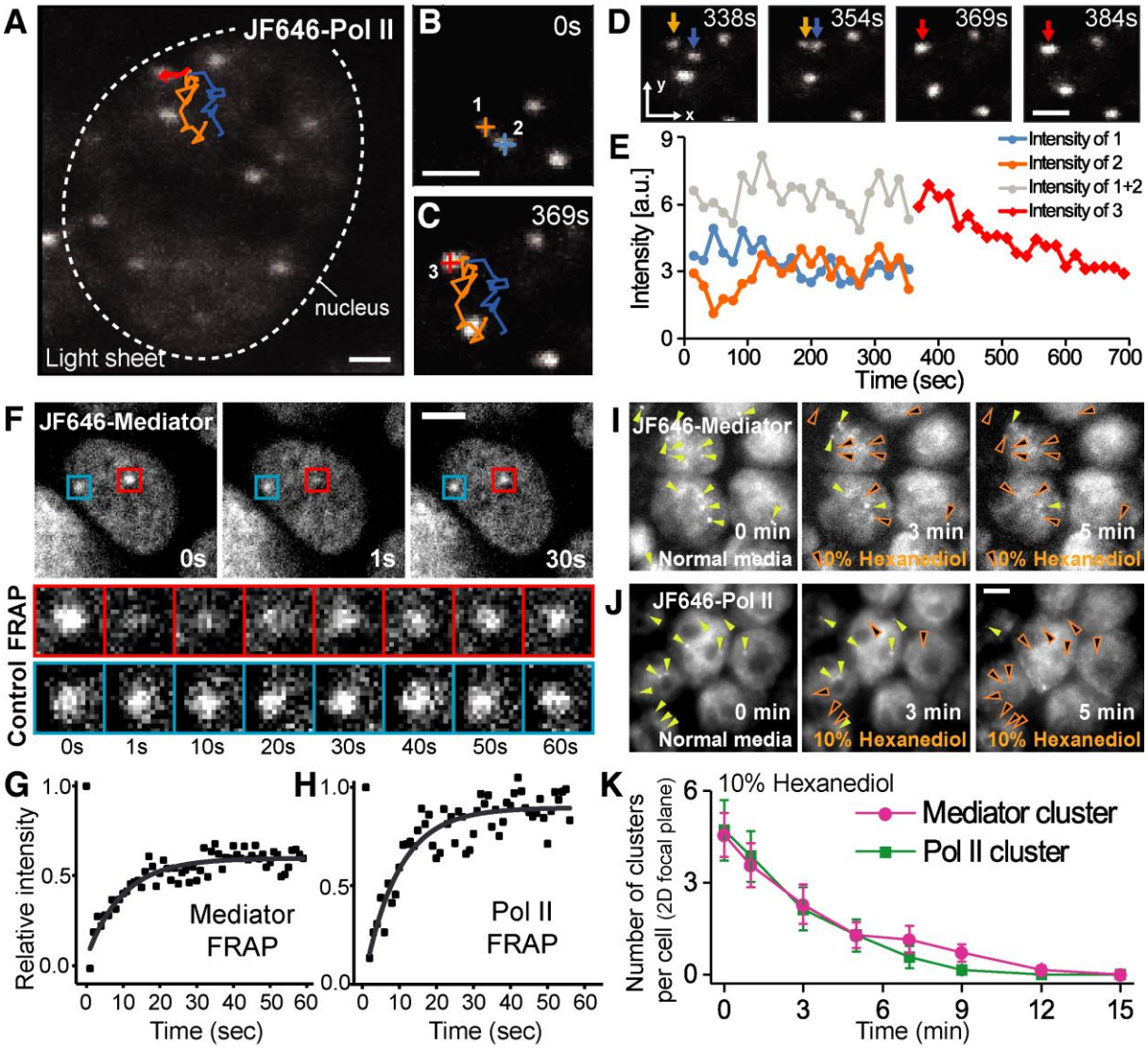

Fig. 3. Mediator and Pol II form condensates that coalesce, recover in FRAP, and are sensitive to hexanediol.

(A-E) Clusters fusion **(A)** Maximum intensity projection of a live cell imaged by lattice light sheet microscopy. Trajectories of two clusters are indicated. (**B, C**) Clusters observed at time 0s fusing at time 369s. (**D**) Individual time points around the fusion event. Orange and blue arrows indicate the precursor clusters, red arrow the fused cluster. (**E**) Time course of the clusters intensities. (**F-H**) FRAP analysis on clusters. (**F**, top panels) Images of a JF646-Mediator cell before (0s, left), immediately after (1s, middle), and 30s after bleaching (right). Red box indicates the position of the cluster on which the FRAP beam was focused. Blue box indicates an unbleached control locus. (**F**, bottom panels) Cropped images as function of time for both loci. (**G**) The normalized recovery curve for Mediator (N=9 cells) yielded a recovery fraction of 60% during the 60s observation with a half recovery time of 10s. (**H**) FRAP on JF646-PolII (N=3 cells) yielded 90% recovery with an identical half recovery time of 10s. (**I, J**) Treatment with 10% hexanediol (v/v) gradually dissolving clusters of JF646-Mediator (top) and JF646-Pol II (bottom). Maximum intensity projection of epifluorescence z-stacks. Yellow arrowheads indicate clusters identified at 0 min. Black arrowheads indicate clusters that disappeared. (**K**) Average number of clusters per cell

(single 2D focal plane) observed in direct imaging as a function of time after hexanediol addition. (N=14 cells for JF646-Mediator, N=14 cells for JF646-Pol II).

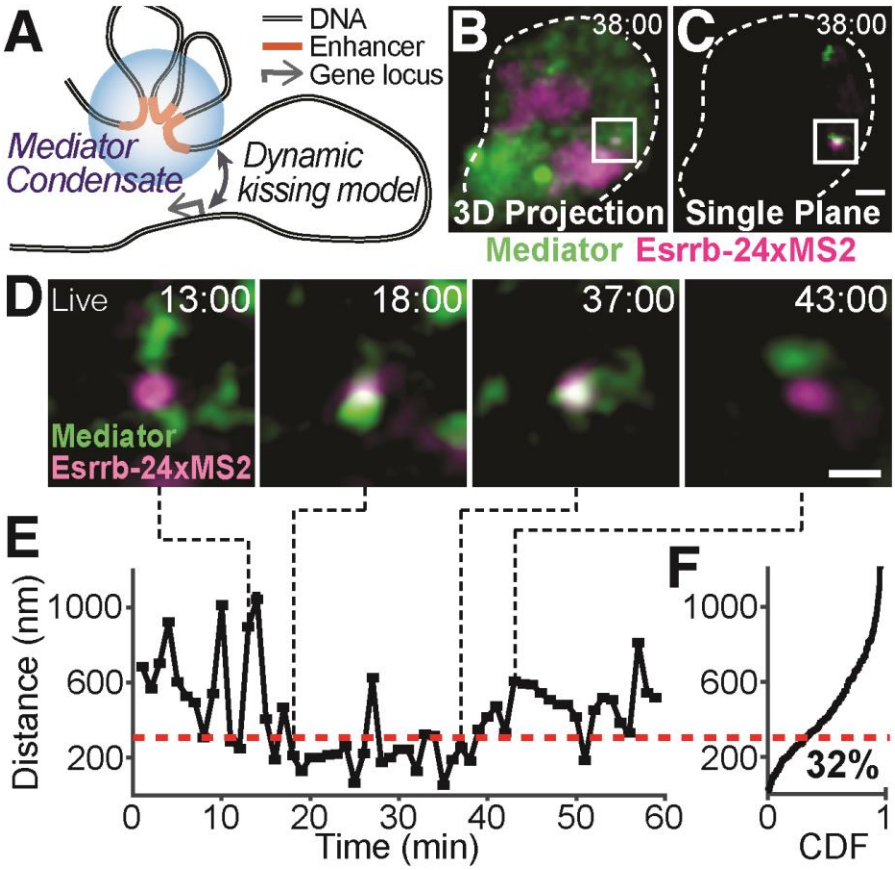

Fig. 4. Mediator clusters dynamically kiss actively transcribing SE-controlled genes.
(**A**) Illustration of the working model describing cluster kissing interaction with a gene locus. (**B**) Maximum intensity projection of a cell imaged using lattice light sheet microscopy showing colocalization of a JF646-Mediator cluster with actively transcribing *Esrrb* gene locus marked by MS2-tagged RNA (white box). (**C**) Single plane from the z stack after background subtraction. (**D**) Snapshot images of a Mediator cluster near the actively transcribing *Essrb* gene locus. (**E**) Plot of the centroid-to-centroid distance from the gene locus to the nearest cluster as a function of time. (**F**) Cumulative distribution of distances from the *Esrrb* locus to the nearest Mediator cluster pooled from N=6 cells (291 time points). Red dashed line in **E** and **F** indicates colocalization threshold (300nm). Scale bars 2μm (**B,C**), 500nm (**D**).